

Sea quark effects in B_K from $N_f = 2$ clover-improved Wilson fermions

Jonathan M. Flynn^a, Federico Mescia^{b,c} and Abdullah Shams Bin Tariq^{a,d}

UKQCD collaboration

^a*School of Physics and Astronomy, University of Southampton,
Southampton, SO17 1BJ, UK*

^b*Dipartimento di Fisica, Univ. degli Studi “Roma TRE”,
via della Vasca Navale 84, I-00146 Roma, Italy*

^c*INFN, Laboratori Nazionali di Frascati, Via E. Fermi 40, I-00044 Frascati, Italy*

^d*Department of Physics, Rajshahi University, Rajshahi 6205, Bangladesh*

*E-mail: j.flynn@hep.phys.soton.ac.uk, mescia@fis.uniroma3.it,
asbt@hep.phys.soton.ac.uk*

ABSTRACT: We report calculations of the parameter B_K appearing in the $\Delta S = 2$ neutral kaon mixing matrix element, whose uncertainty limits the power of unitarity triangle constraints for testing the standard model or looking for new physics. We use two flavours of dynamical clover-improved Wilson lattice fermions and look for dependence on the dynamical quark mass at fixed lattice spacing. We see some evidence for dynamical quark effects and in particular B_K decreases as the sea quark masses are reduced towards the up/down quark mass.

KEYWORDS: Lattice QCD, SM parameters, Kaon physics.

Contents

1. Introduction	1
2. Setup of the calculation	3
3. Numerical simulation	4
4. Analysis and discussion	8
5. Conclusion	12

1. Introduction

B_K is the $\Delta S = 2$ neutral kaon mixing matrix element normalised by its vacuum saturation approximation (VSA) value,

$$B_K(\mu) = \frac{\langle \overline{K^0} | Q^{\Delta S=2}(\mu) | K^0 \rangle}{\frac{8}{3} f_K^2 m_K^2}, \quad (1.1)$$

with μ indicating the scale dependence of the operator $Q(\mu) = \bar{s}\gamma_\mu(1 - \gamma_5)d \bar{s}\gamma^\mu(1 - \gamma_5)d$. This can be related to the one-loop renormalisation group invariant (RGI) value \hat{B}_K through

$$\hat{B}_K = \left[\alpha_s^{(n_f)}(\mu) \right]^{-\frac{\gamma_0}{2\beta_0}} \left[1 + \frac{\alpha_s^{(n_f)}(\mu)}{4\pi} J(n_f) \right] B_K(\mu), \quad (1.2)$$

where n_f is the number of active flavours at the relevant scale, and γ_0 and β_0 have the scheme independent values of 4 and $11 - 2n_f/3$. We use the $\overline{\text{MS}}$ scheme for which J is calculated to NLO in [1]. To go from $\overline{\text{MS}}$ at 2 GeV to the RGI value we note that there are four active flavours and $J_{\overline{\text{MS}}}(4) = 1.792$. Starting from the PDG value of $\Lambda_{\text{QCD}}^{(5)} = 216$ MeV and matching the strong coupling at the charm threshold we obtain $\hat{B}_K = 1.404 B_K(\overline{\text{MS}}, 2 \text{ GeV})$. This is rather insensitive to the value of n_f [2].

The standard model expression for the indirect CP violating parameter [3] as quoted in [4],

$$\varepsilon_K = \bar{\eta} A^2 \hat{B}_K [1.11(5) \cdot A^2(1 - \bar{\rho}) + 0.31(5)], \quad (1.3)$$

defines a hyperbola in the $(\bar{\rho}, \bar{\eta})$ plane, A , $\bar{\rho}$ and $\bar{\eta}$ being parameters of the CKM matrix elements and unitarity triangle [5]. The theoretical uncertainty in the value

	B_K	Fermion	Ren	a^{-1}
	$\overline{\text{MS}}, 2 \text{ GeV}$	Action		(GeV)
Kilcup <i>et al.</i> (1997) [6]	0.62(2)(2)	Staggered	Pert	∞
JLQCD (1997) [7]	0.63(4)	Staggered	Pert	∞
SPQcdR (2002) [8]	0.66(7)	Clover	NP	∞
JLQCD (1999) [9]	0.69(7)	Wilson	NP	∞
CP-PACS (2001) [10]	0.57(1)	DW	Pert	1.8, 2.8
RBC (2002) [11]	0.53(1)	DW	NP	1.9
MILC (2003) [12]	0.55(7)	Overlap	Pert	∞
Garron <i>et al.</i> (2003) [13]	0.63(6)(1)	Overlap	NP	2.1
ALPHA (2003) [14]	0.66(6)(2)	Tw Mass	NP	2.1
RBC (2003) [15]	0.50(2)	Dyn DW	NP	1.8

Table 1: Some previous lattice calculations of B_K . NP refers to non-perturbative renormalisation. Only the last number is unquenched.

of \hat{B}_K remains the dominant uncertainty when we try to use this expression along with the experimental value of ε_K to constrain the triangle. This has resulted in a great deal of activity in the lattice community to refine this calculation.

There is a relatively long history of B_K calculations in different frameworks. Some recent lattice calculations are listed in table 1. A more comprehensive summary can be found in [16], with numbers from other methods dispersed over a relatively wide range. Over the years the quenched lattice value of B_K has more or less settled down. The 1997 quenched value of $B_K(\overline{\text{MS}}, 2 \text{ GeV}) = 0.63(4)$, corresponding to $\hat{B}_K = 0.87(6)$, using staggered fermions [7] remains the benchmark and is the value usually quoted for phenomenology. Other quenched numbers are more or less consistent with this. The error quoted however does not include any estimate for quenching effects and this has been estimated to be as high as 15% [17]. Unquenching remains the primary systematic effect to be addressed.

There has been one preliminary report of a complete unquenched calculation using Domain Wall (DW) fermions from the RBC collaboration [15] and a few other attempts on selected sets of parameters using Wilson and staggered fermions. Though the central values for B_K from DW fermions have often been on the lower side, the unquenched DW preliminary number is really at the lower end of the spectrum. Other attempts to unquench, *e.g.* [4, 18, 19, 20, 21, 22], have not always been able to see a definite effect. However, it has been noted [23] that though the unquenched numbers are consistent with the quenched numbers within errors, they are systematically lower. Hence, it is difficult to reach an unambiguous conclusion on the true effect of dynamical fermions on this quantity.

In this paper, we report on a calculation using two degenerate flavours of dynamical (clover-improved) Wilson fermions. In order to look for sea-quark dependence in

B_K we use three different sea quark masses in the region $m_P/m_V \geq 0.7$ on a volume of $16^3 \times 32$ ($m_P L \geq 7$) but a nearly constant lattice spacing. To achieve the latter a set of values of the bare coupling and bare dynamical quark mass have been chosen in [24, 25] to keep the lattice spacings, defined using the scale r_0 [26], as fixed as possible.

For B_K , we see some evidence for dynamical quark effects and in particular the values decrease as the sea quark mass decreases from the simulated range towards the up/down quark values.

This calculation is undertaken as an intermediate step towards a complete unquenched evaluation of B_K . In the near future one might hope to perform detailed studies over lighter and larger samples of sea quark masses at different lattice spacings in order to make the continuum extrapolation. In the meantime, exploratory studies may help as a guide to those regions of parameters accessible today.

The plan of this paper is as follows. In section 2 we give the basic definitions and in section 3 introduce the quantities relevant for a lattice estimate of B_K . In section 4, we discuss the analysis and present our values and then we have some concluding remarks in the final section.

2. Setup of the calculation

In the continuum, the operator of interest in eq. (1.1) is

$$Q^{\Delta S=2}(\mu) \equiv Q_1(\mu) = \bar{s}\gamma_\mu d \bar{s}\gamma^\mu d + \bar{s}\gamma_\mu\gamma_5 d \bar{s}\gamma^\mu\gamma_5 d, \quad (2.1)$$

which is the parity conserving part of $Q(\mu)$ in eq. (1.1). For Wilson fermions, owing to the breaking of explicit chiral symmetry, there is a mixing of this operator with other four-fermion operators. Therefore one has to work with a complete basis of operators and subtract the extra ones. One such set is

$$\begin{aligned} Q_1(\mu) &= \bar{s}\gamma_\mu d \bar{s}\gamma^\mu d + \bar{s}\gamma_\mu\gamma_5 d \bar{s}\gamma^\mu\gamma_5 d \\ Q_2(\mu) &= \bar{s}\gamma_\mu d \bar{s}\gamma^\mu d - \bar{s}\gamma_\mu\gamma_5 d \bar{s}\gamma^\mu\gamma_5 d \\ Q_3(\mu) &= \bar{s}d \bar{s}d + \bar{s}\gamma_5 d \bar{s}\gamma_5 d \\ Q_4(\mu) &= \bar{s}d \bar{s}d - \bar{s}\gamma_5 d \bar{s}\gamma_5 d \\ Q_5(\mu) &= \bar{s}\sigma_{\mu\nu} d \bar{s}\sigma_{\mu\nu} d. \end{aligned} \quad (2.2)$$

Together with the overall multiplicative renormalisation, the subtraction of the unwanted operators may be expressed in a compact form as

$$Q^{\text{cont}}(\mu) = Z(\mu, g_0^2) \left(Q_1^{\text{latt}} + \sum_{i \neq 1} \Delta_i(g_0^2) Q_i^{\text{latt}} \right). \quad (2.3)$$

The renormalisation coefficients Z and Δ_i have been determined perturbatively for $\overline{\text{MS}}$ -NDR in [27, 28]. Once the renormalisation and subtraction of eq. (2.3) is carried through, we have the matrix element for our desired operator in eq. (1.1).

For fermion implementations which (nearly) respect chiral symmetry, *e.g.* in [6, 11, 13], the chiral behaviour is not modified by lattice artefacts and $B_K(\mu)$ can be obtained from matrix elements of kaons at rest. But for Wilson fermions as, for example, in [4, 18], lattice artefacts introduce chiral symmetry breaking contributions to B_K in the chiral limit. In our case, even though we use an improved-clover action, four-fermion operators are unimproved and $\mathcal{O}(a)$ artefacts may be present. To partially remove them at finite lattice spacing another degree of freedom is required and this can be done by introducing non-zero momentum kaons. Simulations at different lattice spacings and extrapolation to the continuum also allow lattice artefacts to be removed.

Let us now consider matrix elements with non-vanishing external momenta and generic pseudoscalar mesons. On the lattice, the chiral behaviour of the matrix element with non-vanishing external momenta can be parametrised as [17]

$$\langle \bar{P}^0, \vec{p} | Q(\mu) | P^0, \vec{q} \rangle = \alpha' + \beta' m_P^2 + \delta' m_P^4 + (p \cdot q) (\gamma + \gamma' + (\epsilon + \epsilon') m_P^2 + (\xi + \xi')(p \cdot q)) + \dots \quad (2.4)$$

where all the quantities are expressed in lattice units and the ellipsis stands for higher-order terms in $p \cdot q$ and m_P^2 . All the primed coefficients are lattice artefacts. However, while γ' and ϵ' are corrections of $\mathcal{O}(a)$ to the corresponding physical contributions, the parameters α' , β' and δ' are absent in the continuum limit and have to be subtracted from the estimate of B_K in eq. (1.1). In particular the α' term makes B_K divergent in the chiral limit.

For our calculation with Wilson fermions, we neglect higher order terms and use the following expression for the matrix elements:

$$\langle \bar{P}^0, \vec{p} | Q(\mu) | P^0, \vec{q} \rangle = \alpha' + \beta' m_P^2 + (\gamma + \gamma')(p \cdot q). \quad (2.5)$$

3. Numerical simulation

In this work B_K is calculated using Clover-improved Wilson fermions [29] on the UKQCD set of unquenched configurations listed in table 2. Details of the generation of the gauge configurations can be found in [24, 25]. To have a decorrelated sample, configurations separated by 40/50 trajectory steps are used. These configurations are on a lattice of 32×16^3 points.

The lattice spacings determined from the Sommer scale, r_0 , are very similar for these sets. However, there are concerns that the κ_{sea} -dependence of the lattice spacing observed in these configurations is due to the proximity to a phase transition

Set	β	c_{SW}	κ_{sea}	$a(\text{fm})[\text{GeV}^{-1}]$	$(m_P/m_V)_{\kappa_{\text{sea}}=\kappa_{\text{val}}}$	No. of configs
I	5.20	2.0171	0.1350	0.103(2) [1.91(2)]	0.70(1)	100
II	5.26	1.9497	0.1345	0.104(1) [1.90(2)]	0.78(1)	100
III	5.29	1.9192	0.1340	0.102(2) [1.94(2)]	0.83(1)	80

Table 2: The configurations used. Values for lattice spacings are as calculated from the value of the scale, r_0 , in lattice units from the UKQCD set [24, 25].

around $a \simeq 0.1$ fm where there may be large cutoff effects in the dynamical case [30, 31, 32] and therefore needs to be considered with caution. We take the view that, nevertheless, these sets of configurations do have some degree of matching according to a valence-quark-independent definition of an effective lattice spacing, and thus, unless our physics is completely overwhelmed by any nearby phase transition, a combined analysis of the data as a function of κ_{sea} is worthwhile. It may be noted that since B_K is dimensionless, the lattice spacing enters through discretisation errors but not via an overall power of a . Moreover, when analysing the sea quark mass dependence, we use the variable $(am_P)^2(\kappa_{\text{sea}}, \kappa_{\text{sea}})$ which in our case is equivalent to using $(r_0 m_P)^2$ since our lattice spacing is defined through r_0 and $r_0 m_P = (r_0/a) \times am_P$ with (r_0/a) fixed for these lattices [24, 25].

Propagators and correlators were calculated using the FermiQCD [33, 34] code. Five valence quark propagators at $\kappa = 0.1356, 0.1350, 0.1345, 0.1340$ and 0.1335 were generated for each sea quark using the Stabilised Biconjugate Gradient method [35]. Smearing was tried, but since it did not give any significant improvement in the signal, the results presented here are for the local case (see comments in the next section).

To calculate the matrix element on the lattice the standard procedure [36] is followed where we calculate the 3- and 2-point correlation functions

$$\mathcal{C}^{(3)}(t_x, t_y; p_x, p_y; \mu) = \sum_{\vec{x}\vec{y}} \langle P_5(\vec{x}, t_x) Q(\vec{0}; \mu) P_5(\vec{y}, t_y) \rangle e^{i\vec{p}_x \vec{x}} e^{i\vec{p}_y \vec{y}} \quad (3.1)$$

$$\xrightarrow{-t_y, t_x \gg 0} \mathcal{Z}_P e^{-E_x t_x} \langle \bar{P} | Q(\mu) | P \rangle \mathcal{Z}_P e^{-E_y t_y},$$

$$\mathcal{C}_{J_i J_j}^{(2)}(t; p_x) = \sum_{\vec{x}} \langle J_i(\vec{x}, t) J_j^\dagger(0, 0) \rangle e^{i\vec{p}_x \vec{x}} \quad (3.2)$$

$$\xrightarrow{t_x \gg 0} \mathcal{Z}_{J_i} \mathcal{Z}_{J_j} e^{-E_x t}.$$

Here the J 's are kaon interpolating operators and can be of pseudoscalar or axial vector type; they can also be local or smeared. We use pseudoscalar current sources. In the 3-pt functions, the operator is fixed at the origin and t_y is kept fixed at a particular value, while t_x is varied over the full temporal range of the lattice. The main reported results are for $t_y = 10$. We have checked with other neighbouring

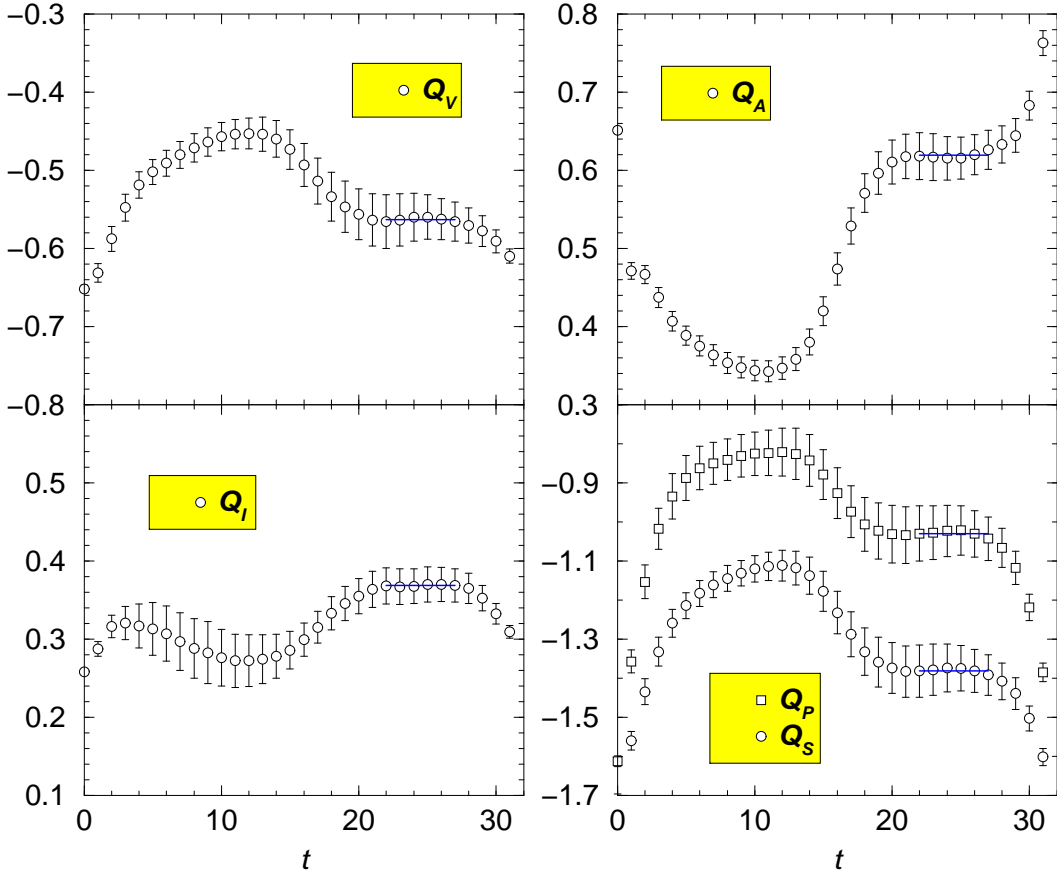


Figure 1: Fits for lattice matrix elements for the complete set of bare operators for a sample of our data (set I, $\kappa_{\text{val}} = 0.1350$). Ratios of the 3-pt correlators to two 2-pt $\langle PP \rangle$ correlators are fitted in the interval $t_x = 22 - 27$ for $t_y = 10$ (see eq. 3.4). Correlators are shown for zero momentum. The fitted ones are those of interest $\langle \bar{P}^0 | Q_i | P^0 \rangle$ while the other plateau in the first half of the lattice corresponds to the $\langle \bar{P}^0 \bar{P}^0 | Q_i | 0 \rangle$ matrix elements.

values of t_y but observe no dependence, implying that the ground state is reasonably well isolated by this time. For the momentum configurations, we have chosen $\{p_x, p_y\} = \{(0, 0, 0), (0, 0, 0)\}, \{(0, 0, 0), (1, 0, 0)\}$ and $\{(1, 0, 0), (0, 0, 0)\}$ where the average over equivalent configurations is understood.

For simulation, we use the simpler basis of

$$\begin{aligned}
Q_V(\mu) &= \bar{s}\gamma_\mu d \bar{s}\gamma^\mu d \\
Q_A(\mu) &= \bar{s}\gamma_\mu\gamma_5 d \bar{s}\gamma^\mu\gamma_5 d \\
Q_I(\mu) &= \bar{s}d \bar{s}d \\
Q_P(\mu) &= \bar{s}\gamma_5 d \bar{s}\gamma_5 d \\
Q_S(\mu) &= \bar{s}\sigma_{\mu\nu} d \bar{s}\sigma_{\mu\nu} d,
\end{aligned} \tag{3.3}$$

which is related to our renormalisation basis introduced in the previous section

Set	g_0^2	$Z(2 \text{ GeV}, g_0^2)$	$Z \Delta_1(g_0^2)$	$Z \Delta_2(g_0^2)$	$Z \Delta_3(g_0^2)$	$Z \Delta_4(g_0^2)$	Z_A
I	2.162	0.4959	-0.0385	-0.0070	0.0140	0.0140	0.7482
II	2.113	0.5072	-0.0376	-0.0068	0.0137	0.0137	0.7540
III	2.091	0.5133	-0.0372	-0.0068	0.0135	0.0135	0.7565

Table 3: Perturbative matching coefficients to go from $B_K^{\text{latt}}(\mu = 1/a)$ to $B_K^{\overline{\text{MS}}}(\mu = 2 \text{ GeV})$.

through a simple rotation. Fitted ratios for this basis that give us the matrix elements in lattice units, Q_i^{latt} , ($i = V, A, I, P, S$) are plotted in fig. 1.

To go directly to $\overline{\text{MS}}$ at $\mu = 2 \text{ GeV}$, we note that in our case $(a\mu) \approx 1$ and we can naively use standard perturbation theory at one-loop. For the coupling there is a range of choices that may lead to different numerical values. We use the boosted bare lattice coupling, $g_0^2 = 6/\beta\langle P \rangle$, where $\langle P \rangle$ is value of the relevant average plaquette and our values are $\{0.5336, 0.5399, 0.5424\}$. For c_{SW} the one-loop value of 1.0 is used. The perturbative matching coefficients thus obtained are listed in table 3.

To extract the desired matrix element the following ratios are formed:

$$R_3 = \frac{\mathcal{C}^{(3)}(t_x, t_y; p_x, p_y; \mu)}{Z_A^2 \mathcal{C}_{PP}^{(2)}(t_x; p_x) \mathcal{C}_{PP}^{(2)}(t_y; p_y)} \longrightarrow \frac{1}{Z_A^2 Z_P^2} \langle \bar{P}^0, \vec{p}_x | Q(\mu) | P^0, \vec{p}_y \rangle, \quad (3.4)$$

$$X(0) = \frac{8}{3} \left| \frac{\mathcal{C}_{A_0P}^{(2)}(t_x)}{\mathcal{C}_{PP}^{(2)}(t_x)} \right|^2 \longrightarrow \frac{1}{Z_A^2 Z_P^2} \frac{8}{3} f_P^2 m_P^2, \quad (3.5)$$

$$X(\vec{p}) = X(0) \cdot \frac{(p_x \cdot p_y)}{m_P^2} \longrightarrow \frac{1}{Z_A^2 Z_P^2} \frac{8}{3} f_P^2 (p_x \cdot p_y), \quad (3.6)$$

where Z_A is the axial current renormalisation.

At this stage one may fit the equation

$$R_3 = \tilde{\alpha}' + \tilde{\beta}' X(0) + (\tilde{\gamma} + \tilde{\gamma}') X(\vec{p}), \quad (3.7)$$

with

$$\tilde{\alpha}' \equiv \frac{\alpha'}{Z_A^2 Z_P^2}, \quad \tilde{\beta}' \equiv \frac{3\beta'}{8f_P^2}, \quad \tilde{\gamma} \equiv \frac{3\gamma}{8f_P^2} \quad \text{and} \quad \tilde{\gamma}' \equiv \frac{3\gamma'}{8f_P^2},$$

to obtain estimates for B_K from $\tilde{\gamma}$ [8, 37], by neglecting $\tilde{\gamma}'$. In the fit, the parameters with tildes are taken to be constant and hence the estimates are for effective values of Z_P and f_P in our range of simulation. In this manner, for a set of different valence quarks with a given sea quark mass, this approach gives an estimate of the leading term in an expansion of B_K for that set with the kaons not necessarily being at the physical kaon mass.

To obtain estimates of B_K for each $(\kappa_{\text{sea}}, \kappa_{\text{val}})$ combination, which will then allow us to extrapolate in the quark masses, we follow the approach of [18, 27].

Let us call the non-zero- and zero-momentum R_3 's $R_3(\vec{p})$ and $R_3(0)$ respectively, corresponding to $X(\vec{p})$ and $X(0)$ defined in eq. 3.4. The two non-zero momenta $\{p_x, p_y\} = \{(0, 0, 0), (1, 0, 0)\}$ and $\{(1, 0, 0), (0, 0, 0)\}$, have been averaged, since they are estimates of the same matrix elements in the continuum and indeed numerically are found to be very similar. Then we have

$$\left. \frac{R_3(\vec{p}) - R_3(0)}{X(\vec{p}) - X(0)} \right|_{(\kappa_{\text{sea}}, \kappa_{\text{val}})} = B_K(\mu, \kappa_{\text{sea}}, \kappa_{\text{val}}). \quad (3.8)$$

These can then be used in our chiral extrapolations in the sea and valence quarks. At the same time, fitting these values to a constant for a given sea quark is similar to estimating $\tilde{\gamma}$ from a fit of eq. 3.7. At higher orders of momentum, this expression differs from the correct dependence of B_K by a term like $\tilde{\xi} m_P E(\vec{p})$ [27]. We have found the coefficient $\tilde{\xi}$ of this term difficult to determine, particularly for our limited set of momenta. However, if we were able to make this correction, it would simply change our values of B_K within our systematics, leaving our conclusions unchanged.

4. Analysis and discussion

The values obtained for $B_K(\overline{\text{MS}}, 2 \text{ GeV})$ for our sets of masses are tabulated in table 4. We refer to the ones quoted from eq. (3.7) following [8, 37] and from eq. (3.8) following [18, 27] as method I and II respectively.

We have degenerate valence quarks. So, SU(3) breaking effects due to $m_s \neq m_{u,d}$ are not accounted for. Rather our kaon is made up of two quarks around $m_s/2$. Moreover, the results in table 4 are obtained for local sources. Indeed, we have not seen any significant improvement of the signal from smearing. This is not unexpected since we have a local operator at the origin and can smear only at the sink, which is usually less effective than source smearing. It may also be due to a lack of optimisation of the smearing parameters. However, results were fully compatible with those using local operators and we have restricted the presentation to the simpler case.

In fig. 2, we plot $B_K(\overline{\text{MS}}, 2 \text{ GeV})$ from method II as a function of the corresponding squared pseudoscalar masses over the complete set of our valence and sea quark masses. We observe the points for the lightest valence quarks diverging for the different sea quarks. Here, it may be noted that for $\kappa_{\text{val}} \gg \kappa_{\text{sea}}$ the theory becomes more like quenched. This effect is clearly seen in fig. 3 of [38] where as the valence quark becomes lighter the partially quenched curves leave the full theory and tend towards the quenched one. Finite volume effects are, in general, expected to be small [39], but for some regions of parameter space, particularly for very light quarks, it has been suggested that finite volume effects can obscure the chiral behaviour in B_K [38]. The JLQCD collaboration [40] observes finite volume effects for lighter sea quarks for the same action, but for our parameters they have excluded finite volume effects

$(\beta, \kappa_{\text{sea}})$	κ_{val}	m_P/m_V	$(am_P)^2$	Method I	Method II
				$B_K(\kappa_{\text{sea}})$	$B_K(\kappa_{\text{sea}}, \kappa_{\text{val}})$
(5.20, 0.1350)	0.1356	0.62(3)	0.106(5)	0.64(7)	0.41(12)
	0.1350	0.72(2)	0.166(4)		0.57(9)
	0.1345	0.77(1)	0.218(4)		0.63(7)
	0.1340	0.80(1)	0.270(4)		0.66(6)
	0.1335	0.83(1)	0.324(4)		0.69(5)
(5.26, 0.1345)	0.1356	0.67(2)	0.151(3)	0.69(8)	0.70(16)
	0.1350	0.74(1)	0.206(3)		0.71(10)
	0.1345	0.77(1)	0.255(3)		0.71(8)
	0.1340	0.81(1)	0.306(4)		0.72(7)
	0.1335	0.83(1)	0.359(4)		0.72(6)
(5.29, 0.1340)	0.1356	0.72(2)	0.170(5)	0.79(4)	0.81(6)
	0.1350	0.77(1)	0.229(5)		0.79(4)
	0.1345	0.80(1)	0.280(5)		0.78(4)
	0.1340	0.83(1)	0.332(6)		0.77(4)
	0.1335	0.85(1)	0.386(6)		0.77(4)

Table 4: Simulated values of $B_K(\overline{\text{MS}}, 2 \text{ GeV})$. Method I refers to a direct fit of eq. (3.7); while in method II, eq. (3.8) is used to obtain values for each $(\kappa_{\text{sea}}, \kappa_{\text{val}})$ combination.

for pseudoscalar meson correlators down to just beyond our lightest point in set I. Indeed we find the finite volume correction from [38] to be -0.1% for this point. Nonetheless, we note that, contrary to the other sets, for set I, the $\mathcal{O}(a)$ discretisation error parameters $\tilde{\alpha}$ and $\tilde{\beta}$ turn out to have finite values of $-0.06(2)$ and $0.23(8)$. The effects of these terms are greater at lighter quark masses and we cannot be sure that the curvature observed here is due to a true chiral behaviour. As can be seen from our values of m_P/m_V , this point is at a considerably lighter mass than all the other points. Therefore, we choose to be cautious and exclude it from our analysis. It would be interesting to know if non-perturbative renormalisation [41, 42], and/or the improvement programme of [43, 44] could lead to better chiral behaviour.

Now let us consider the values from method I. It is notable that for these rather heavy sea quarks these numbers are compatible with quenched estimates. This is the reason that previous attempts to unquench for a fixed heavy sea quark mass have found it difficult to disentangle the unquenching effects.

Since we have more than one sea quark mass in our simulation, we can attempt to extrapolate these numbers to the chiral limit. We use a linear fit versus the unitary pseudoscalar masses $(am_P)^2(\kappa_{\text{sea}} = \kappa_{\text{val}})$ and go to the up/down limit. This gives us

$$B_K(\overline{\text{MS}}, 2 \text{ GeV}) = 0.49(13), \quad (4.1)$$

which corresponds to $\hat{B}_K = 0.69(18)$.

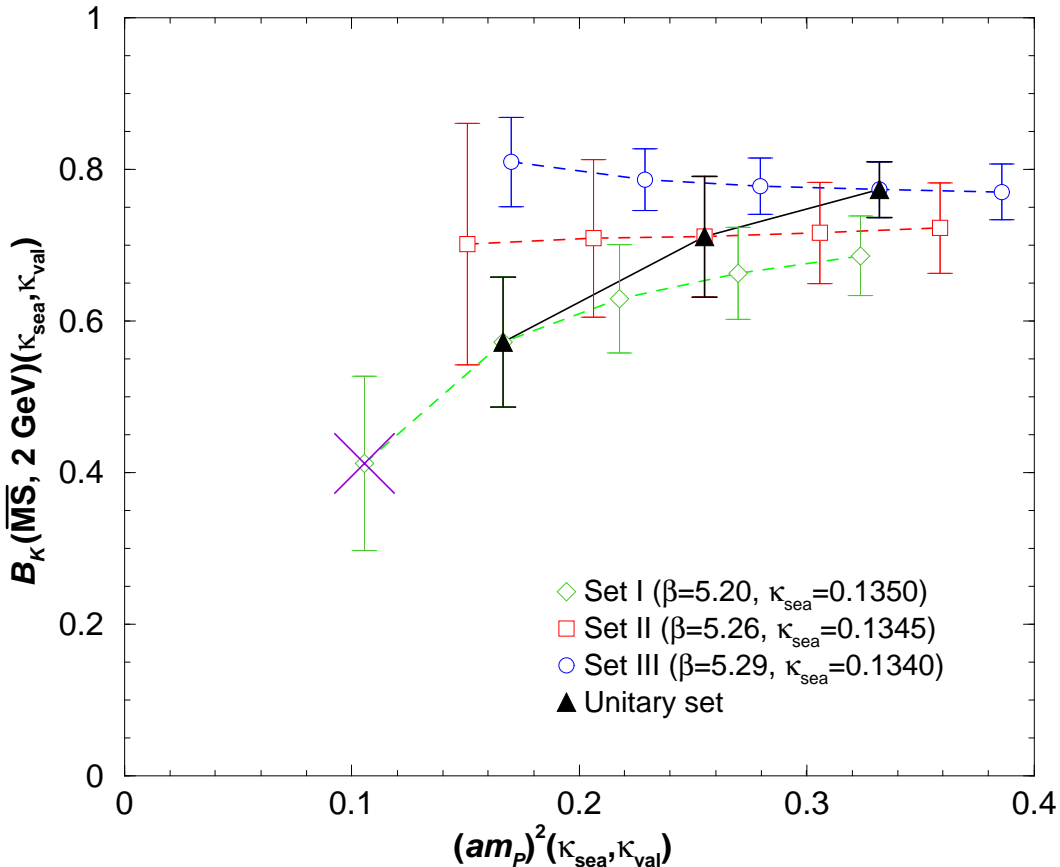


Figure 2: Values of $B_K(\overline{\text{MS}}, 2 \text{ GeV})$ for each $(\kappa_{\text{sea}}, \kappa_{\text{val}})$ combination plotted as a function of the corresponding squared pseudoscalar masses. The dashed lines joining the points are just for a visual guide separating the sets with different sea quarks. The filled points joined by a solid line are the unitary ones for which $\kappa_{\text{sea}} = \kappa_{\text{val}}$. The lightest point for set I (marked by a large cross) is excluded from the analysis.

In this method we estimate $\tilde{\gamma}$ in eq. 3.7. As mentioned in the previous section, the valence quarks are not necessarily such that $m_P = m_K^{\text{phys}}$. In fact one can note by comparing with the last column of table 4 that these values are in the simulated region. Therefore one may think of this estimate as one of B_K where the sea quarks are realistically light but the valence quarks are heavier than the physical strange quark.

A somewhat complementary approach, would be to follow the route of [15] and take the unitary points, *i.e.* the points with $\kappa_{\text{sea}} = \kappa_{\text{val}}$ from method II, for extrapolation to the physical kaon mass [fig. 4]. This leads to

$$B_K(\overline{\text{MS}}, 2 \text{ GeV}) = 0.48(13), \quad (4.2)$$

Corresponding to $\hat{B}_K = 0.67(18)$. Here we have a more reasonable valence $m_P = m_K^{\text{phys}}$, but on the other hand the sea and valence quarks are degenerate and hence

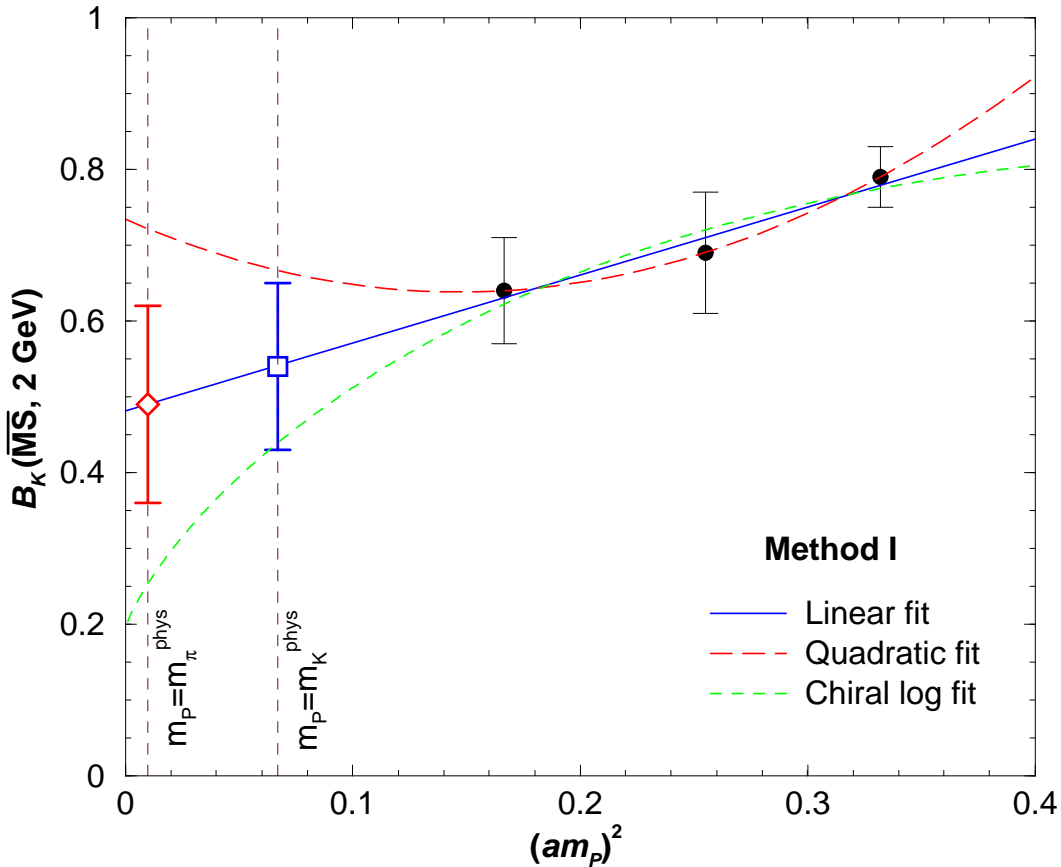


Figure 3: Fit to the data from method I. The values quoted is from the linear extrapolation, whereas the quadratic and chiral log-type fits are added for illustration. The extrapolated points at $m_P = m_\pi^{\text{phys}}$ and $m_P = m_K^{\text{phys}}$ are also shown.

the sea content is not as light as the up/down quarks. To understand how much this may affect us we note that if we take all the quark masses (both valence and sea) to zero our value of B_K goes down to $0.40(17)$ and $\hat{B}_K = 0.56(24)$.

A combined analysis of valence and sea quarks has been tried for the spectroscopy studies in [25, 40]. With more momenta, higher statistics and/or a larger sample of sea and valence quark masses and if the higher order terms in B_K could be estimated, this would be a possible route to an estimate of B_K at the physical valence and sea masses.

Even though we recognise that the presence of several artefacts does not allow a quantitative estimate of the sea quark dependence, it does seem that dynamical quark effects can be quite significant. There also seem to be indications that, incorporating dynamical quarks lowers the value of B_K . Taking this together with the observation in [23] that the $N_f = 2$ numbers are always lower than those for $N_f = 0$, a statement also valid for subsequent works, we see that when one has two finite-mass but still heavy sea quarks, B_K starts to decrease but is still consistent with the quenched

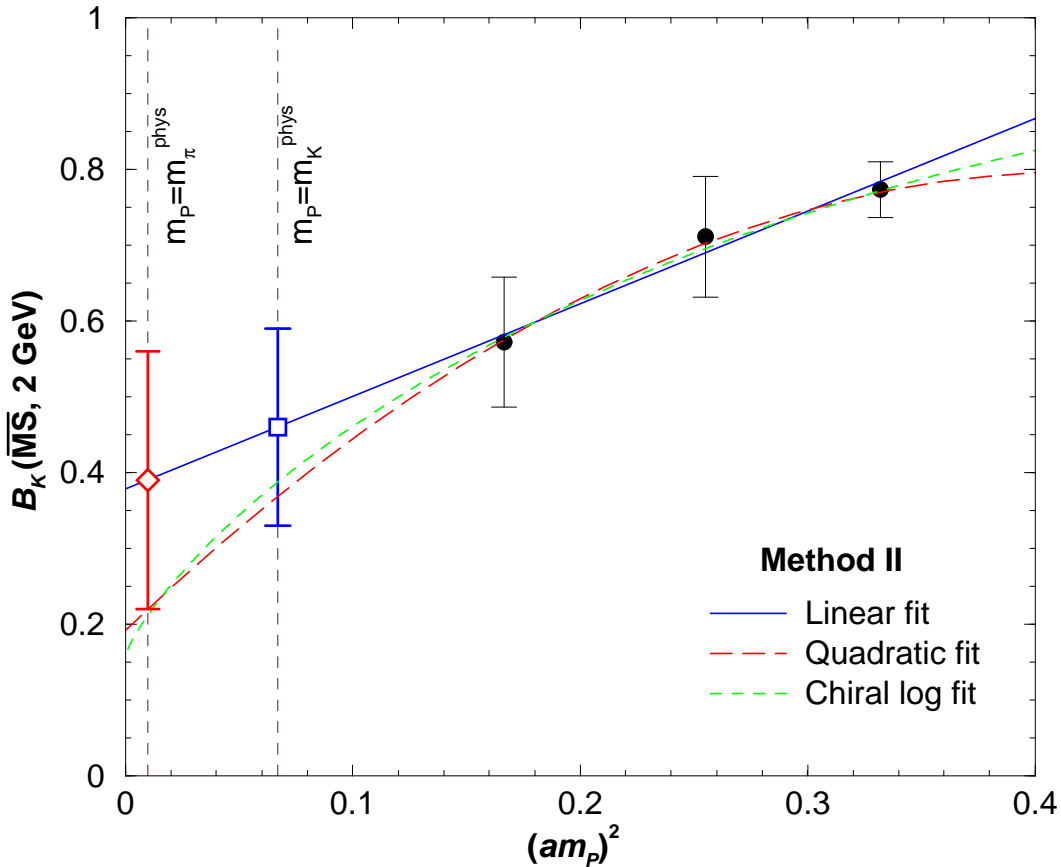


Figure 4: Unitary fit of the data. The value quoted is from the linear extrapolation, whereas the quadratic and chiral log-type fits are added for illustration. The vertical lines show the positions where $m_P = m_\pi^{\text{phys}}$ and $m_P = m_K^{\text{phys}}$, respectively.

value within errors. When the sea quarks can be taken to the massless limit, the value of B_K becomes distinctly lower than the quenched result. It is also intriguing to note that in a recent study where \hat{B}_K is taken as a free parameter and fitted using the other unitarity triangle constraints, the value obtained is $\hat{B}_K = 0.69(11)$ [45], again lower than the usual quenched lattice value.

Owing to the exploratory nature of our analysis and large statistical errors, a study of systematic errors such as those connected to choices of fit window, chiral extrapolation, renormalisation method, the fixed time at one end, the strong coupling, Λ_{QCD} , etc. has not been addressed.

5. Conclusion

We have presented results for B_K calculated using non-perturbatively $\mathcal{O}(a)$ -improved Wilson fermions with two dynamical flavours for three sets of relatively small volume lattices of matched spacing. Despite some concern about the robustness of the

estimates due to various lattice uncertainties, there are indications that dynamical quark effects are important and lead to a lower value of B_K .

Acknowledgments

We would like to thank Massimo Di Pierro for his help in using the FermiQCD code. We also thank the Iridis parallel computing team at University of Southampton, in particular, Ivan Wolton, Ian Hardy and Oz Parchment for their computing support. We thank Damir Becirevic, Ken Bowler, Martin Hasenbusch, Alan Irving, Laurent Lellouch, David Lin, Vittorio Lubicz, Craig McNeile, Chris Michael, Amarjit Soni and Giovanni Villadoro for their comments. The work of ASBT is supported by a Commonwealth Scholarship. Work partially supported by the European Community's Human Potential Programme under HPRN-CT-2000-00145 Hadrons/Lattice QCD. FM is also partially supported by IHP-RTN, EC contract no. HPRN-CT-2002-00311 (EURIDICE).

References

- [1] M. Ciuchini *et. al.*, *Next-to-leading order QCD corrections to $\Delta F = 2$ effective Hamiltonians*, *Nucl. Phys.* **B523** (1998) 501–525, [[hep-ph/9711402](#)].
- [2] D. Becirevic, *Lattice results relevant to the CKM matrix determination*, [hep-ph/0211340](#).
- [3] G. Buchalla, A. J. Buras, and M. E. Lautenbacher, *Weak decays beyond leading logarithms*, *Rev. Mod. Phys.* **68** (1996) 1125–1144, [[hep-ph/9512380](#)].
- [4] D. Becirevic, D. Meloni, and A. Retico, *An estimate of the $K^0 - \overline{K}^0$ mixing amplitude*, *JHEP* **01** (2001) 012, [[hep-lat/0012009](#)].
- [5] L. Wolfenstein, *Parametrization of the Kobayashi-Maskawa matrix*, *Phys. Rev. Lett.* **51** (1983) 1945.
- [6] G. Kilcup, R. Gupta, and S. R. Sharpe, *Staggered fermion matrix elements using smeared operators*, *Phys. Rev.* **D57** (1998) 1654–1665, [[hep-lat/9707006](#)].
- [7] **JLQCD** Collaboration, S. Aoki *et. al.*, *Kaon B parameter from quenched lattice QCD*, *Phys. Rev. Lett.* **80** (1998) 5271–5274, [[hep-lat/9710073](#)].
- [8] **SPQCDR** Collaboration, D. Becirevic *et. al.*, *Kaon weak matrix elements with Wilson fermions*, *Nucl. Phys. Proc. Suppl.* **119** (2003) 359–361, [[hep-lat/0209136](#)].
- [9] **JLQCD** Collaboration, S. Aoki *et. al.*, *The kaon B-parameter with the Wilson quark action using chiral Ward identities*, *Phys. Rev.* **D60** (1999) 034511, [[hep-lat/9901018](#)].

- [10] **CP-PACS** Collaboration, A. Ali Khan *et. al.*, *Kaon B parameter from quenched domain-wall QCD*, *Phys. Rev.* **D64** (2001) 114506, [[hep-lat/0105020](#)].
- [11] **RBC** Collaboration, T. Blum *et. al.*, *Kaon matrix elements and CP-violation from quenched lattice QCD. I: The 3-flavor case*, *Phys. Rev.* **D68** (2003) 114506, [[hep-lat/0110075](#)].
- [12] **MILC** Collaboration, T. DeGrand, *Kaon B parameter in quenched QCD*, *Phys. Rev.* **D69** (2004) 014504, [[hep-lat/0309026](#)].
- [13] N. Garron, L. Giusti, C. Hoelbling, L. Lellouch, and C. Rebbi, *B_K from quenched QCD with exact chiral symmetry*, *Phys. Rev. Lett.* **92** (2004) 042001, [[hep-ph/0306295](#)].
- [14] **ALPHA** Collaboration, P. Dimopoulos, J. Heitger, C. Pena, S. Sint, and A. Vladikas, *B_K from twisted mass QCD*, [hep-lat/0309134](#).
- [15] **RBC** Collaboration, T. Izubuchi, *B_K from two-flavor dynamical domain wall fermions*, [hep-lat/0310058](#).
- [16] R. Gupta, *Status of B_K from lattice QCD*, [hep-lat/0303010](#).
- [17] S. R. Sharpe, *Chiral perturbation theory and weak matrix elements*, *Nucl. Phys. Proc. Suppl.* **53** (1997) 181–198, [[hep-lat/9609029](#)].
- [18] R. Gupta, D. Daniel, G. W. Kilcup, A. Patel, and S. R. Sharpe, *The Kaon B parameter with Wilson fermions*, *Phys. Rev.* **D47** (1993) 5113–5127, [[hep-lat/9210018](#)].
- [19] G. Kilcup, D. Pekurovsky, and L. Venkataraman, *On the N_f and a dependence of B_K* , *Nucl. Phys. Proc. Suppl.* **53** (1997) 345–348, [[hep-lat/9609006](#)].
- [20] N. Ishizuka *et. al.*, *Viability of perturbative renormalization factors in lattice QCD calculation of the $K^0 - \bar{K}^0$ mixing matrix*, *Phys. Rev. Lett.* **71** (1993) 24–26.
- [21] G. Kilcup, *Effect of quenching on the kaon B parameter*, *Phys. Rev. Lett.* **71** (1993) 1677–1679.
- [22] W.-J. Lee and M. Klomfass, *Numerical study of $K^0 - \bar{K}^0$ mixing and B_K* , [hep-lat/9608089](#).
- [23] A. Soni, *Weak matrix elements on the lattice - circa 1995*, *Nucl. Phys. Proc. Suppl.* **47** (1996) 43–58, [[hep-lat/9510036](#)].
- [24] **UKQCD** Collaboration, A. C. Irving, *Effects of non-perturbatively improved dynamical fermions in UKQCD simulations*, *Nucl. Phys. Proc. Suppl.* **94** (2001) 242–245, [[hep-lat/0010012](#)].

- [25] **UKQCD** Collaboration, C. R. Allton *et. al.*, *Effects of non-perturbatively improved dynamical fermions in QCD at fixed lattice spacing*, *Phys. Rev.* **D65** (2002) 054502, [[hep-lat/0107021](#)].
- [26] R. Sommer, *A New way to set the energy scale in lattice gauge theories and its applications to the static force and α_s in $SU(2)$ Yang-Mills theory*, *Nucl. Phys.* **B411** (1994) 839–854, [[hep-lat/9310022](#)].
- [27] R. Gupta, T. Bhattacharya, and S. R. Sharpe, *Matrix elements of 4-fermion operators with quenched Wilson fermions*, *Phys. Rev.* **D55** (1997) 4036–4054, [[hep-lat/9611023](#)].
- [28] S. Capitani *et. al.*, *Perturbative renormalization of improved lattice operators*, *Nucl. Phys. Proc. Suppl.* **63** (1998) 874–876, [[hep-lat/9709049](#)].
- [29] M. Luscher, S. Sint, R. Sommer, P. Weisz, and U. Wolff, *Non-perturbative $O(a)$ improvement of lattice QCD*, *Nucl. Phys.* **B491** (1997) 323–343, [[hep-lat/9609035](#)].
- [30] **ALPHA, CP-PACS and JLQCD** Collaboration, R. Sommer *et. al.*, *Large cutoff effects of dynamical Wilson fermions*, [hep-lat/0309171](#).
- [31] **ALPHA** Collaboration, M. Della Morte, R. Hoffmann, F. Knechtli, and U. Wolff, *Impact of large cutoff-effects on algorithms for improved Wilson fermions*, [hep-lat/0405017](#).
- [32] M. Hasenbusch, private communication.
- [33] M. Di Pierro, *FermiQCD: A tool kit for parallel lattice QCD applications*, *Nucl. Phys. Proc. Suppl.* **106** (2002) 1034–1036, [[hep-lat/0110116](#)].
- [34] M. Di Pierro, *Matrix distributed processing and FermiQCD*, [hep-lat/0011083](#).
- [35] A. Frommer, V. Hannemann, B. Nockel, T. Lippert, and K. Schilling, *Accelerating Wilson fermion matrix inversions by means of the stabilized biconjugate gradient algorithm*, *Int. J. Mod. Phys.* **C5** (1994) 1073–1088, [[hep-lat/9404013](#)].
- [36] M. B. Gavela *et. al.*, *The Kaon B parameter and K - π and K - $\pi\pi$ transition amplitudes on the lattice*, *Nucl. Phys.* **B306** (1988) 677.
- [37] M. Crisafulli *et. al.*, *Chiral behaviour of the lattice B_K -parameter with the Wilson and Clover Actions at $\beta = 6.0$* , *Phys. Lett.* **B369** (1996) 325–334, [[hep-lat/9509029](#)].
- [38] D. Becirevic and G. Villadoro, *Impact of the finite volume effects on the chiral behavior of f_K and B_K* , [hep-lat/0311028](#).
- [39] S. R. Sharpe, *Quenched chiral logarithms*, *Phys. Rev.* **D46** (1992) 3146–3168, [[hep-lat/9205020](#)].

- [40] **JLQCD** Collaboration, S. Aoki *et. al.*, *Light hadron spectroscopy with two flavors of $O(a)$ -improved dynamical quarks*, *Phys. Rev.* **D68** (2003) 054502, [[hep-lat/0212039](#)].
- [41] G. Martinelli, C. Pittori, C. T. Sachrajda, M. Testa, and A. Vladikas, *A general method for nonperturbative renormalization of lattice operators*, *Nucl. Phys.* **B445** (1995) 81–108, [[hep-lat/9411010](#)].
- [42] A. Donini, V. Gimenez, G. Martinelli, M. Talevi, and A. Vladikas, *Non-perturbative renormalization of lattice four-fermion operators without power subtractions*, *Eur. Phys. J.* **C10** (1999) 121–142, [[hep-lat/9902030](#)].
- [43] R. Frezzotti and G. C. Rossi, *Chirally improving Wilson fermions. I: $O(a)$ improvement*, [hep-lat/0306014](#).
- [44] R. Frezzotti and G. C. Rossi, *Chirally improving Wilson fermions*, *Nucl. Phys. Proc. Suppl.* **129-130** (2004) 880–882, [[hep-lat/0309157](#)].
- [45] M. Ciuchini *et. al.*, *Unitarity triangle analysis in the standard model and sensitivity to new physics*, *ECONF* **C0304052** (2003) WG306, [[hep-ph/0307195](#)].